# Electronic Supplementary Information

## Sensitivity improvement induced by thermal-response behavior for temperature sensing application

Youfusheng Wu, [ab] Fengqin Lai, [a] Bin Liu, [a] Jianhui Huang, [ab] Xinyu Ye [bc] and Weixiong You *[ab]

[a] *School of Material Science and Engineering, Jiangxi University of Science and Technology, Ganzhou*

*341000, P.R. China;*

[b] *Key Laboratory of Rare Earth Luminescence Materials and Devices of Jiangxi Province, Ganzhou*

*341000, P.R. China;*

[c] *School of Metallurgy and Chemistry Engineering, Jiangxi University of Science and Technology,*

*Ganzhou 341000, P.R. China;*

* Corresponding author. E-mail: you_wx@126.com (W. X. You)，Tel：+86-7978312422

## Part I. Experimental detail

The polycrystal $Ba(Gd_{0.83}Er_{0.05}Yb_{0.12})_2ZnO_5$, $Ba_5(Gd_{0.83}Er_{0.05}Yb_{0.12})_8Zn_4O_{21}$ and their mixture samples were prepared via a high-temperature solid-state method using the starting reagents: $BaCO_3$ (99.99%), $Gd_2O_3$ (99.99%), $Er_2O_3$ (99.99%), $Yb_2O_3$ (99.99%) and ZnO (AR), and all raw materials were used without further purification. According to the chemical composition, the starting materials were handled with the order of calculation, weight and grind. As for the mixture sample, the dosages of raw materials were calculated separately but ground and sintered in a mixed situation. At last, the grounded mixtures were calcined at $1300^o$ C for 5 h. White powers were collected for further characterizations.

**Part II Structural information of the NLMW host**

The NLMW host, belonging to the double perovskite family, has a typical perovskite structure ($ABO_3$) in which Na and La atoms occupy the A-site and Mg and W atoms take up the B-site.[1] Figure S1 shows the result of Rietveld refinement of the NLMW host. The precise cell parameters and atomic positions based on those believable factors with $W_{Rp}$ = 8.21%, $R_p$ = 5.35% and $\chi^2$ = 1.681 are revealed and illustrated in Table S1, which is close to the previous report.[2] The NLMW host features a monoclinic structure with space group *C2/m* (Z = 4). To further understand the structural information, Figure S2 presents the crystal structure diagrams along the a-axis and b-axis directions. Obviously, the Na atoms are surrounded by four oxygens, which have two distinct Na–O bands that build two orthogonal flats, to form tetrahedrons. Those La atoms are coordinated by eight oxygens to build polyhedrons and the coordinative atoms are shared with neighboring La atoms through a corner-sharing method. Besides, the atoms at B-site containing Mg and W atoms are coordinated by six oxygens to form the octahedrons that connected via the bridging oxygen atoms.
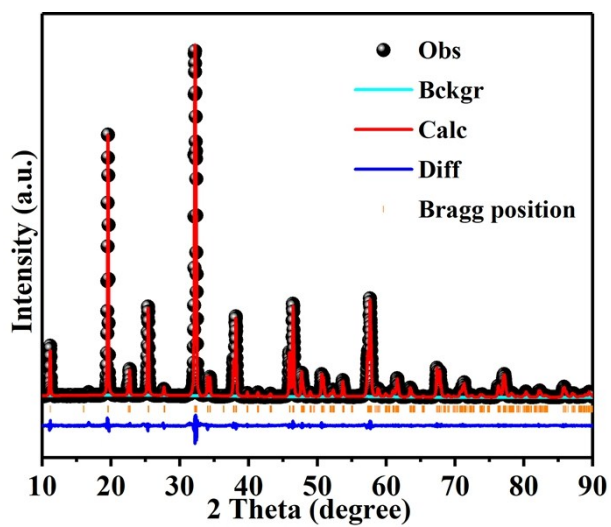
## Part III. Experimental figures and tables



Fig. S1 The Rietveld refinement XRD pattern of the NLMW host.

Table S1 Rietveld refinement parameters of the NLMW host.

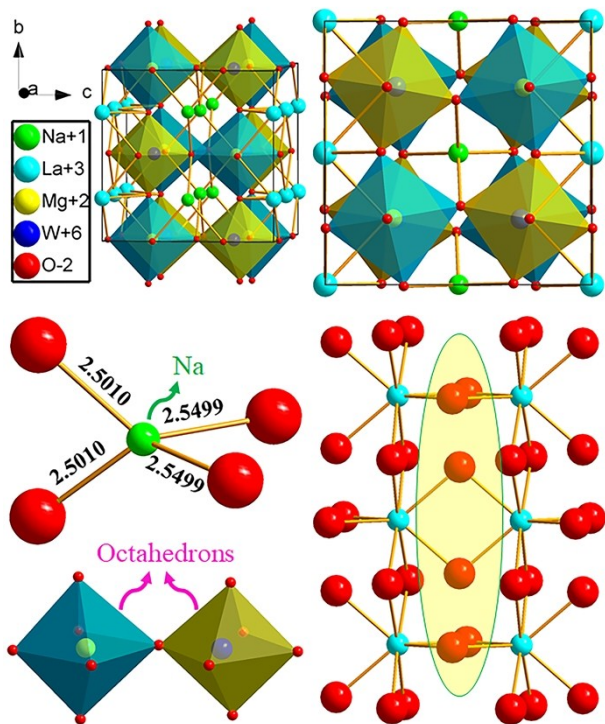| Parameters | Standard card | NLMW host |
|---|---|---|
| a (Å) | 7.8074 (1) | 7.8054 (8) |
| b (Å) | 7.8158 (1) | 7.8159 (5) |
| c (Å) | 7.8977 (1) | 7.8923 (8) |
| α = γ (°) | 90 | 90 |
| β(°) | 90.136 | 90.1192 |
| V (Å$^3$) | 481.92 | 481.492 |
| WRp | | 8.21% |
| Rp | | 5.35% |
| χ$^2$ | | 1.681 |

Fig. S2 Structural diagrams and coordination of information in the NLMW host.
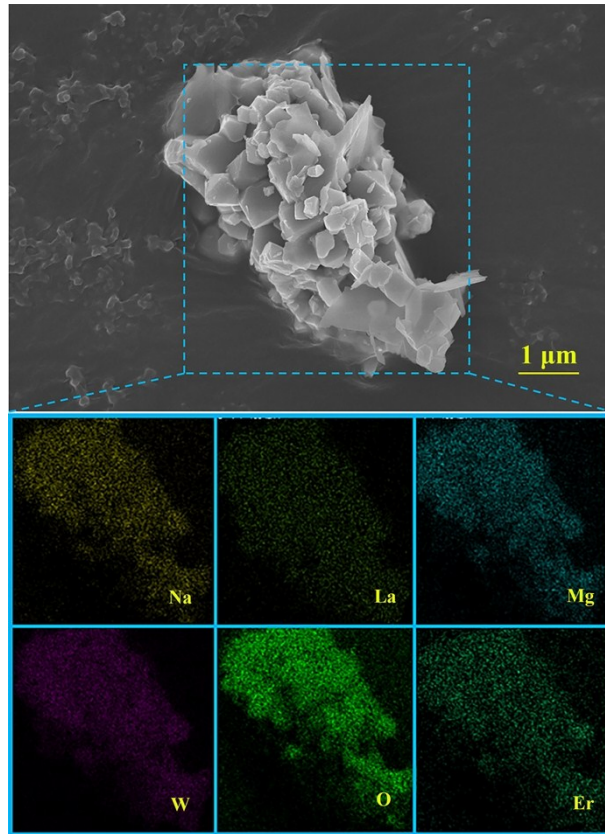
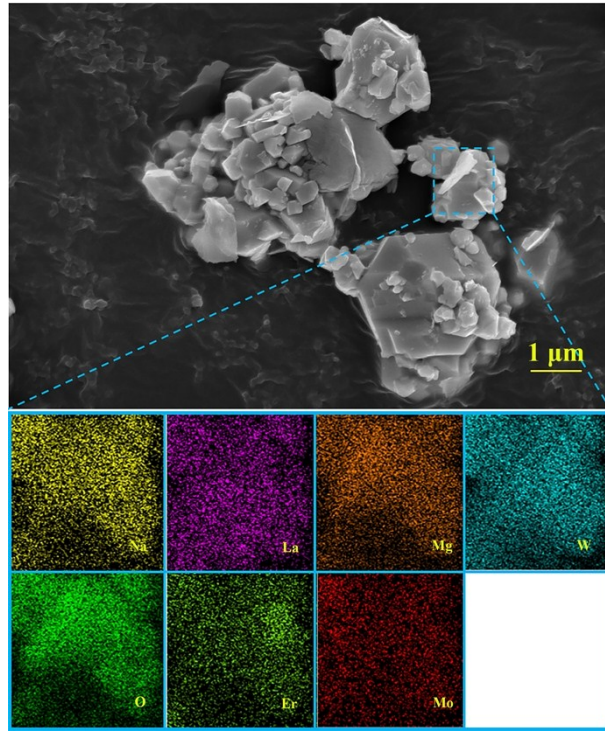Fig. S3 The morphology and elemental mapping images of the NLMW:5%Er$^{3+}$ sample.

Fig. S4 The morphology and elemental mapping images of the NLMW:5%$Er^{3+}$/20%$Mo^{6+}$ sample.
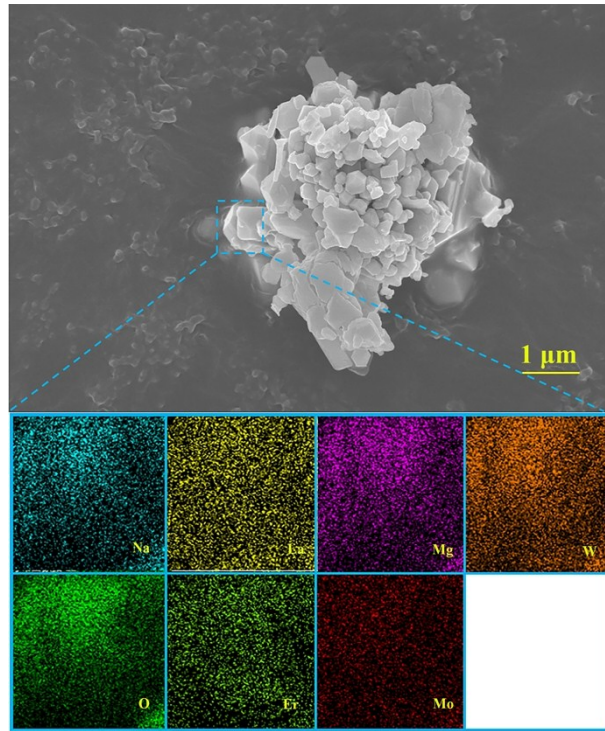
Fig. S5 The morphology and elemental mapping images of the NLMW:5%Er$^{3+}$/40%Mo$^{6+}$ sample.

Fig. S6 FIR (a) – (c) and Ln[FIR] (d) – (f) versus the temperature in those $H/S_1$, $H/S_2$ and H/S parts, and fitting lines following equation (1) and (2) of the NLMW:5%Er$^{3+}$ sample.
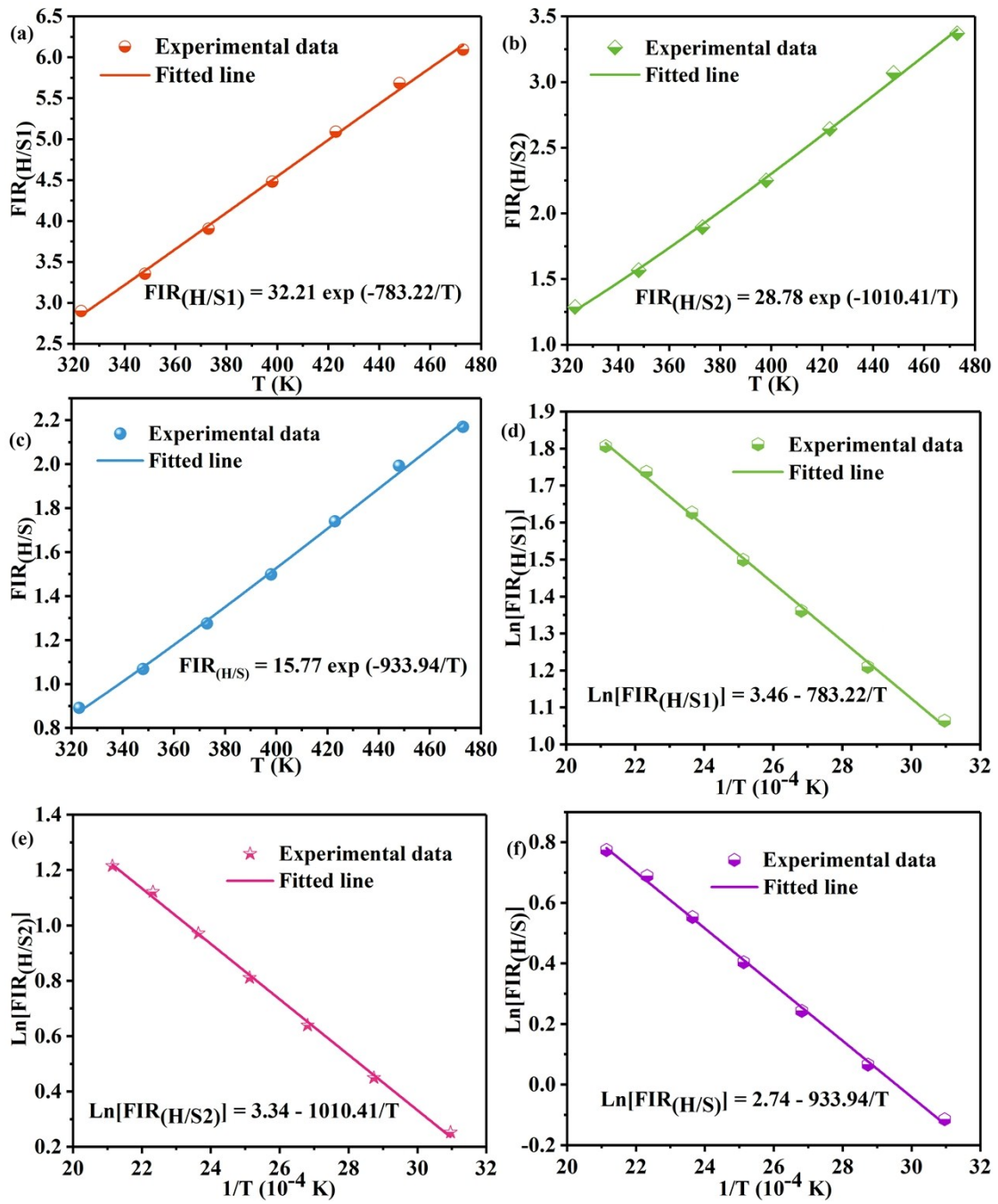
Fig. S7 FIR (a) – (c) and Ln[FIR] (d) – (f) versus the temperature in those $H/S_1$, $H/S_2$ and H/S parts, and fitting lines

following equation (1) and (2) of the NLMW:5%$Er^{3+}$/20%$Mo^{6+}$ sample.
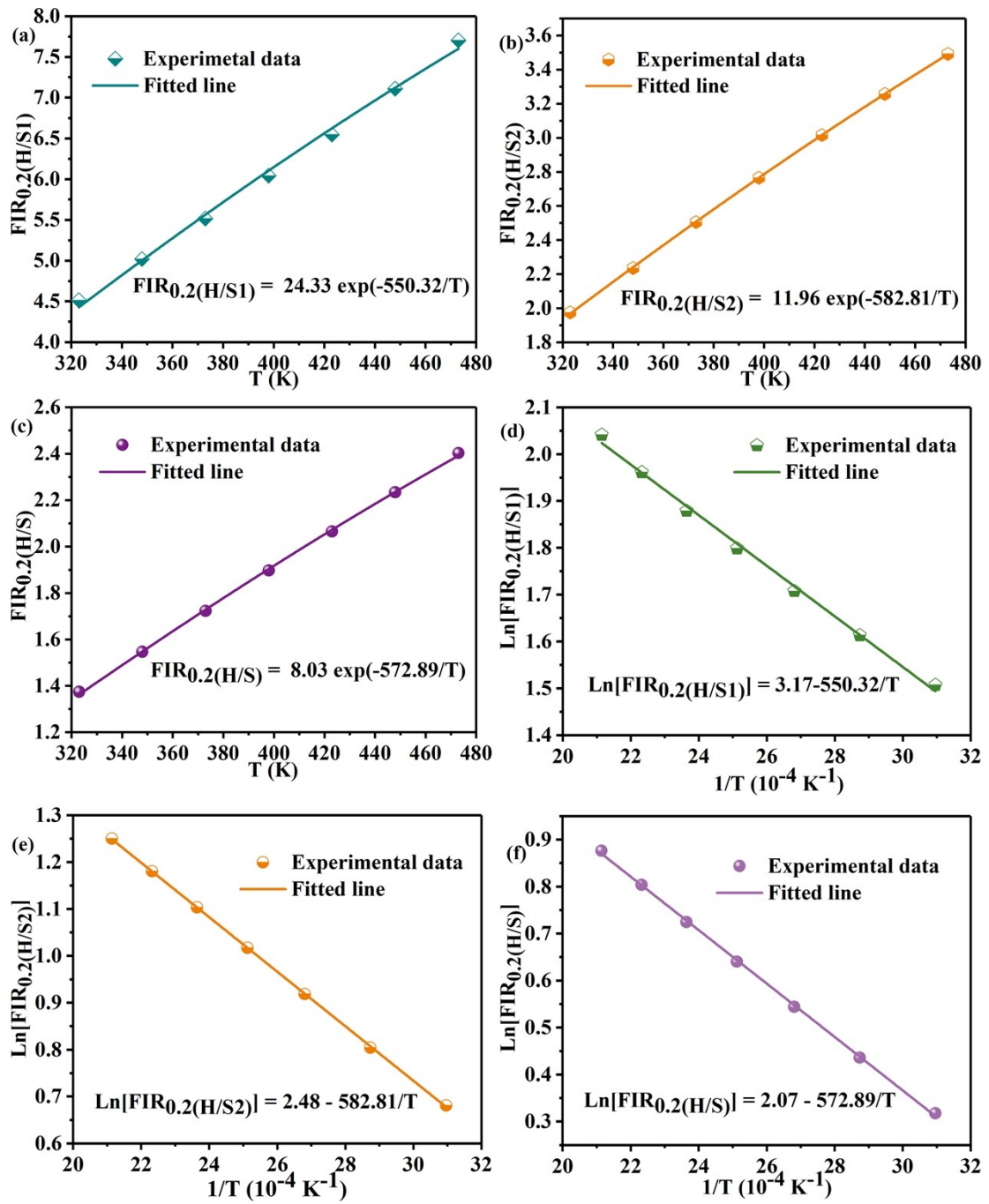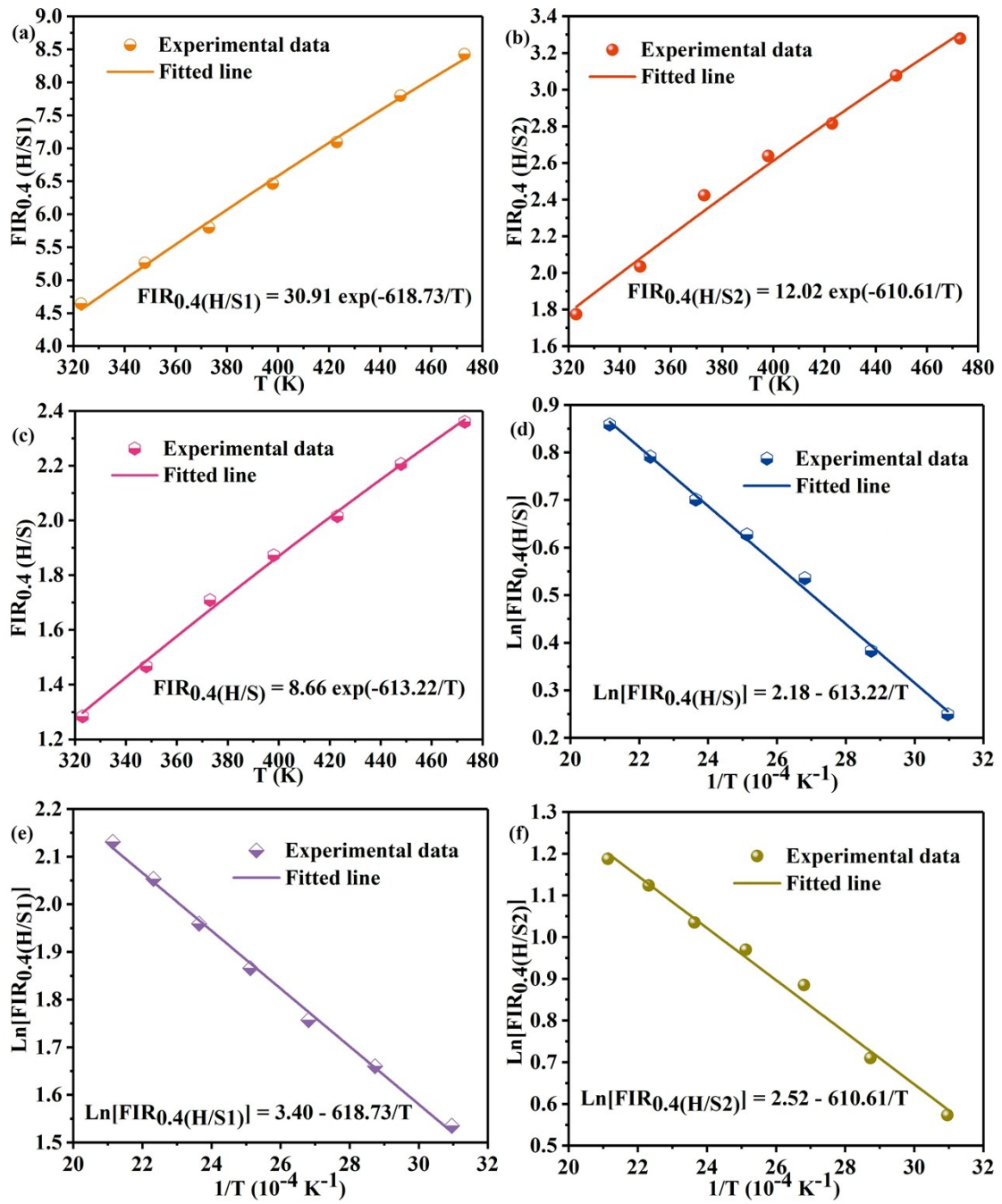
Fig. S8 FIR (a) – (c) and Ln[FIR] (d) – (f) versus the temperature in those $H/S_1$, $H/S_2$ and H/S parts, and fitting lines

following equation (1) and (2) of the NLMW:5%$Er^{3+}$/40%$Mo^{6+}$ sample.

Table S2 Detailed $S_A$ values as a function of the temperature in the NLMW:5%Er$^{3+}$, NLMW:5%Er$^{3+}$/20%Mo$^{6+}$ and NLMW:5%Er$^{3+}$/40%Mo$^{6+}$ samples.

| Mo$^{6+}$ contents | FIR | 323 K | 348 K | 373 K | 398 K | 423 K | 448 K | 473 K |
|---|---|---|---|---|---|---|---|---|
| 0% | H/S$_1$ | 217.7 | 216.9 | 219.7 | 221.5 | 222.8 | 221.8 | 213.3 |
| | H/S$_2$ | 124.7 | 130.8 | 137.6 | 143.6 | 149.3 | 154.5 | 152.5 |
| | H/S | 79.8 | 82.4 | 85.6 | 88.3 | 90.8 | 92.7 | 90.6 |
| 20% | H/S$_1$ | 238.1 | 228.1 | 218.3 | 210.0 | 201.4 | 195.0 | 189.5 |
| | H/S$_2$ | 110.4 | 107.6 | 105.0 | 101.8 | 98.2 | 94.6 | 91.0 |
| | H/S | 75.5 | 73.2 | 71.0 | 68.6 | 66.1 | 63.8 | 61.5 |
| 40% | H/S$_1$ | 275.4 | 268.8 | 257.8 | 252.4 | 245.3 | 240.3 | 233.0 |
| | H/S$_2$ | 103.8 | 102.6 | 106.4 | 101.7 | 96.1 | 93.6 | 89.5 |
| | H/S | 75.5 | 74.3 | 75.3 | 72.5 | 69.1 | 67.4 | 64.7 |

Table S3 Detailed $S_R$ values as a function of the temperature in the NLMW:5%Er$^{3+}$, NLMW:5%Er$^{3+}$/20%Mo$^{6+}$ and NLMW:5%Er$^{3+}$/40%Mo$^{6+}$ samples.

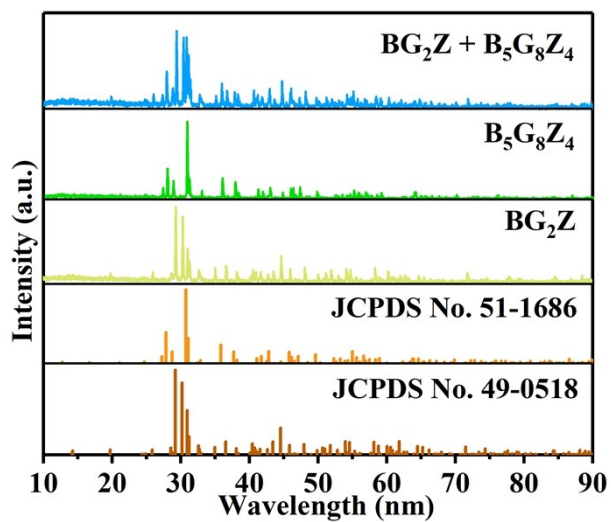| Mo$^{6+}$ contents | FIR | 323 K | 348 K | 373 K | 398 K | 423 K | 448 K | 473 K |
|---|---|---|---|---|---|---|---|---|
| 0% | H/S$_1$ | 7.5 | 6.4 | 5.6 | 4.9 | 4.4 | 3.9 | 3.5 |
| | H/S$_2$ | 9.7 | 8.3 | 7.3 | 6.4 | 5.7 | 5.0 | 4.5 |
| | H/S | 8.9 | 7.7 | 6.7 | 5.9 | 5.2 | 4.7 | 4.2 |
| 20% | H/S$_1$ | 5.3 | 4.5 | 4.0 | 3.5 | 3.1 | 2.7 | 2.5 |
| | H/S$_2$ | 5.6 | 4.8 | 4.2 | 3.7 | 3.3 | 2.9 | 2.6 |
| | H/S | 5.5 | 4.7 | 4.1 | 3.6 | 3.2 | 2.9 | 2.6 |
| 40% | H/S$_1$ | 5.9 | 5.1 | 4.5 | 3.9 | 3.5 | 3.1 | 2.8 |
| | H/S$_2$ | 5.9 | 5.0 | 4.4 | 3.9 | 3.4 | 3.0 | 2.7 |
| | H/S | 5.9 | 5.1 | 4.4 | 3.9 | 3.4 | 3.1 | 2.7 |

Fig. S9 XRD patterns of the $BG_2Z$, $B5G_8Z4$ and the mixture samples
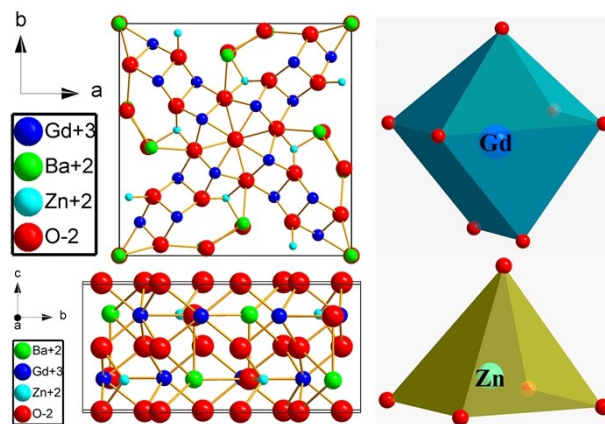
Fig. S10 Structural diagrams and coordination of information for the $BG_2Z$ and $B_5G_8Z_4$ hosts.
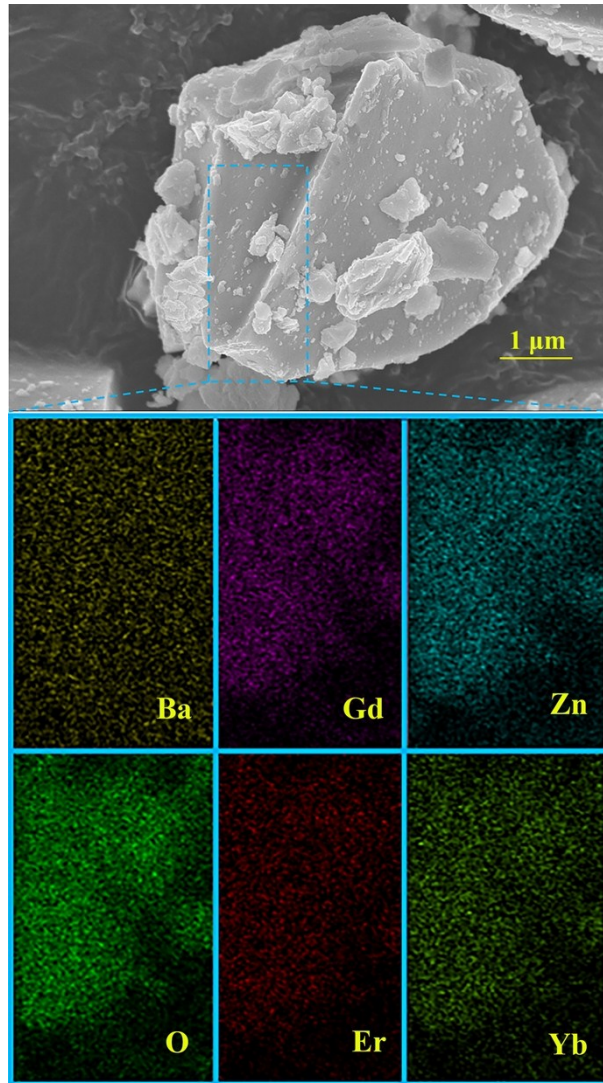
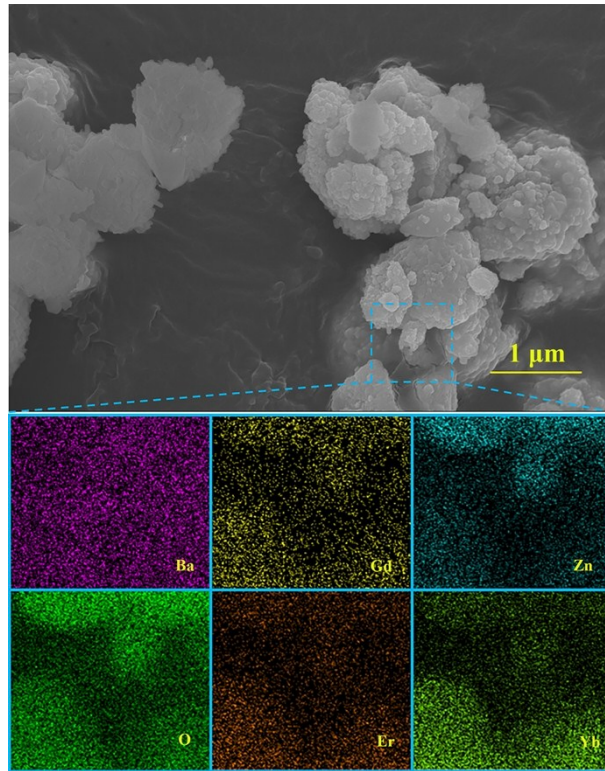Fig. S11 The morphology and elemental mapping images of the BG$_2$Z sample.

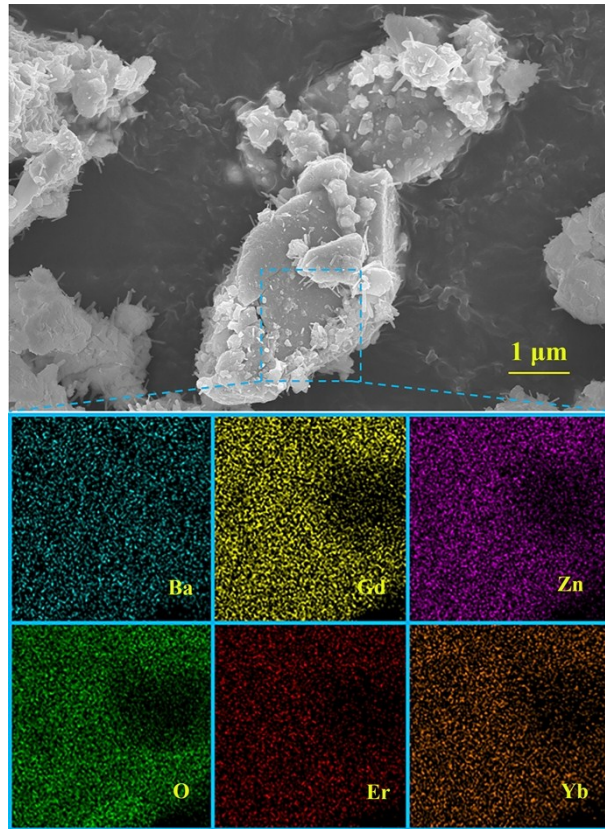Fig. S12 The morphology and elemental mapping images of the $B_5G_8Z_4$ sample.

Fig. S13 The morphology and elemental mapping images of the mixture sample.

Fig. S14 FIR (a) – (c) and Ln[FIR] (d) – (f) versus the temperature in those $H/S_1$, $H/S_2$ and H/S parts, and fitting lines

following equation (1) and (2) of the $BG_2Z$ sample.
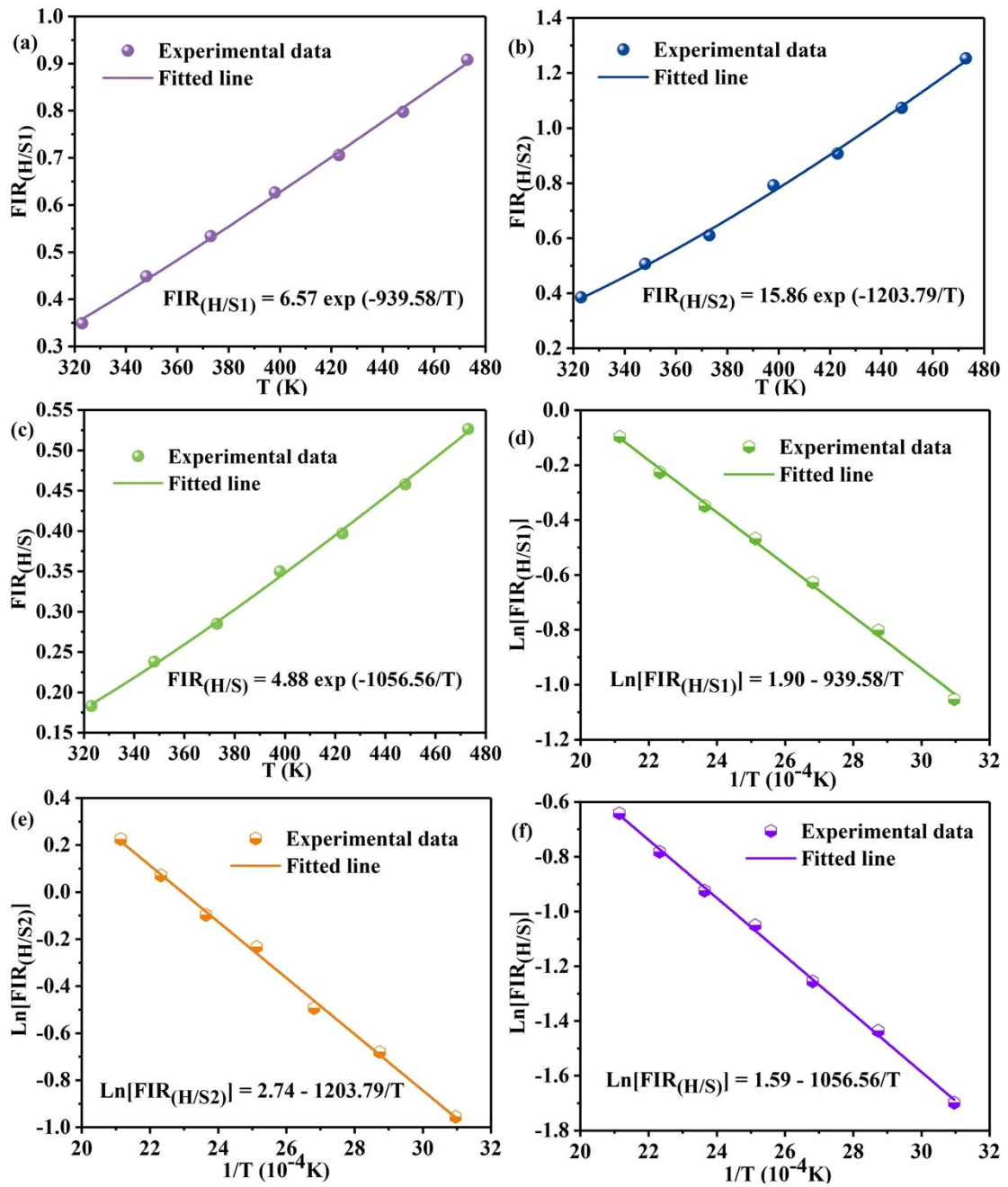
Fig. S15 FIR (a) – (c) and Ln[FIR] (d) – (f) versus the temperature in those $H/S_1$, $H/S_2$ and H/S parts, and fitting lines

following equation (1) and (2) of the $B_5G_8Z_4$ sample.

Fig. S16 FIR (a) – (c) and Ln[FIR] (d) – (f) versus the temperature in those H/S$_1$, H/S$_2$ and H/S parts, and fitting lines

following equation (1) and (2) of the mixture sample.
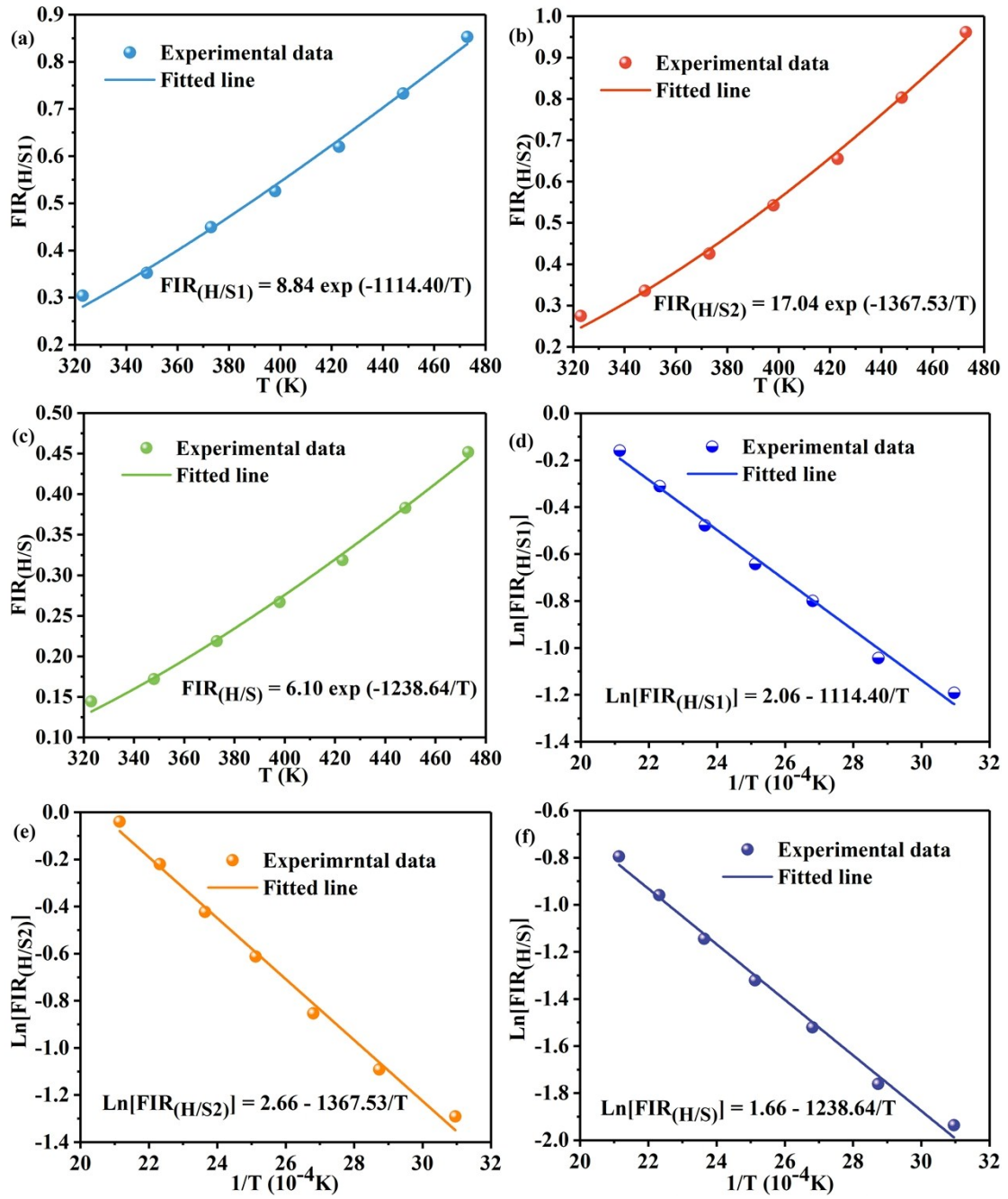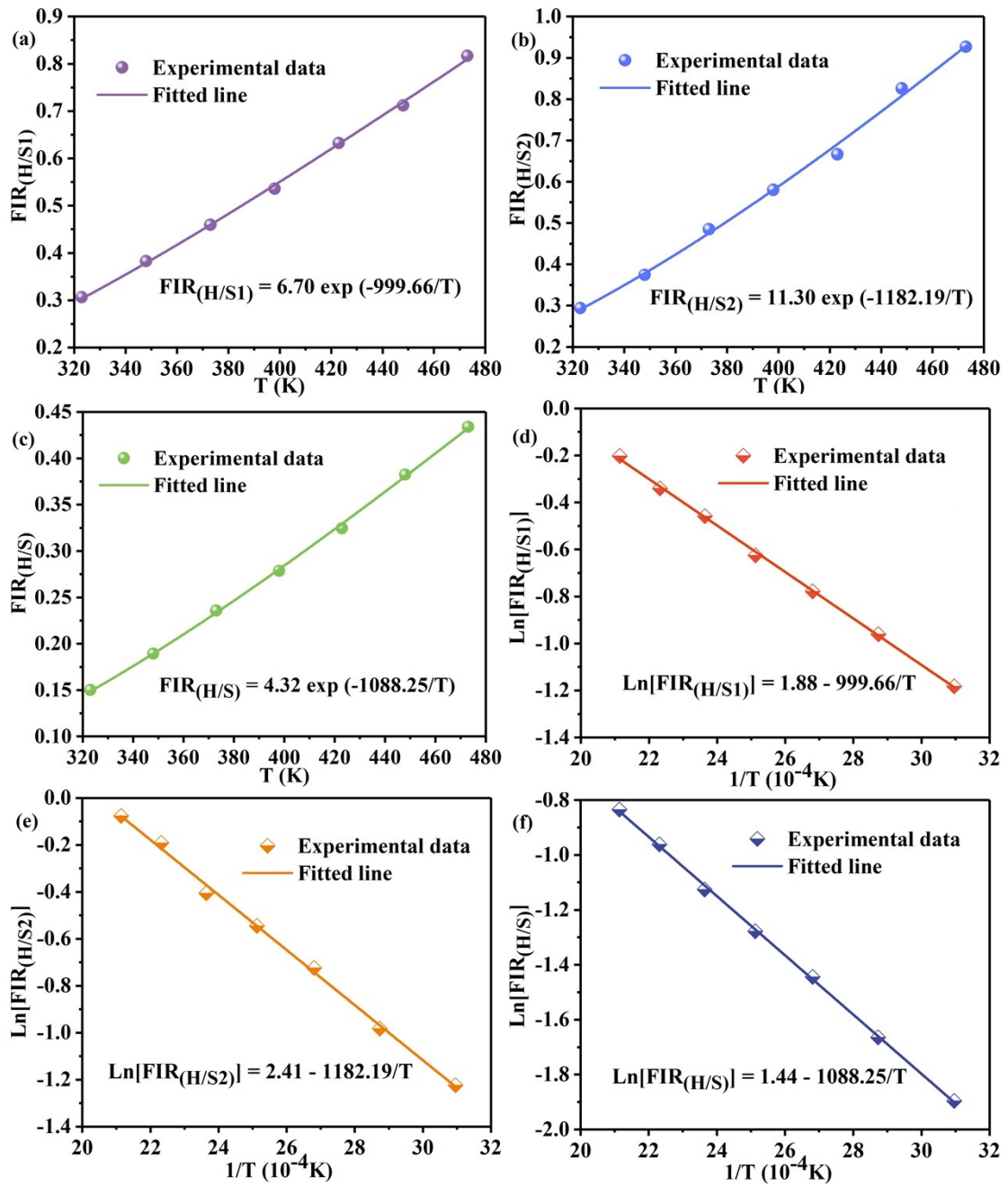
Table S4 Detailed $S_A$ values as a function of the temperature in $BG_2Z$, $B_5G_8Z_4$ and the mixture samples.

| Sample | FIR | 323 K | 348 K | 373 K | 398 K | 423 K | 448 K | 473 K |
|---|---|---|---|---|---|---|---|---|
| | $H/S_1$ | 31.4 | 34.8 | 36.1 | 37.2 | 37.1 | 37.3 | 38.1 |
| $BG_2Z$ | $H/S_2$ | 44.4 | 50.4 | 52.8 | 60.2 | 61.1 | 64.4 | 67.4 |
| | $H/S$ | 18.5 | 20.8 | 21.6 | 23.3 | 23.4 | 24.1 | 24.9 |
| | $H/S_1$ | 32.4 | 32.4 | 36.0 | 37.0 | 38.6 | 40.7 | 42.5 |
| $B_5G_8Z_4$ | $H/S_2$ | 36.0 | 37.9 | 41.9 | 46.8 | 50.1 | 54.7 | 58.7 |
| | $H/S$ | 17.1 | 17.6 | 19.5 | 20.9 | 22.1 | 23.6 | 25.0 |
| $BG_2Z$ | $H/S_1$ | 29.4 | 31.6 | 33.0 | 33.8 | 35.3 | 35.5 | 36.5 |
| $+ B_5G_8Z_4$ | $H/S_2$ | 33.3 | 36.6 | 41.2 | 43.3 | 44.0 | 48.7 | 49.0 |
| | $H/S$ | 15.7 | 17.0 | 18.4 | 19.1 | 19.7 | 20.7 | 21.1 |

Table S5 Detailed $S_R$ values as a function of the temperature in $BG_2Z$, $B_5G_8Z_4$ and the mixture samples.

| Sample | FIR | 323 K | 348 K | 373 K | 398 K | 423 K | 448 K | 473 K |
|---|---|---|---|---|---|---|---|---|
| | $H/S_1$ | 9.0 | 7.8 | 6.8 | 5.9 | 5.3 | 4.7 | 4.2 |
| $BG_2Z$ | $H/S_2$ | 11.5 | 9.9 | 8.7 | 7.6 | 6.7 | 6.0 | 5.4 |
| | $H/S$ | 10.1 | 8.7 | 7.6 | 6.7 | 5.9 | 5.3 | 4.7 |
| | $H/S_1$ | 10.7 | 9.2 | 8.0 | 7.0 | 6.2 | 5.6 | 5.0 |
| $B_5G_8Z_4$ | $H/S_2$ | 13.1 | 11.3 | 9.8 | 8.6 | 7.6 | 6.8 | 6.1 |
| | $H/S$ | 11.9 | 10.2 | 8.9 | 7.8 | 6.9 | 6.2 | 5.5 |
| $BG_2Z$ | $H/S_1$ | 9.6 | 8.3 | 7.2 | 6.3 | 5.6 | 5.0 | 4.5 |
| $+ B_5G_8Z_4$ | $H/S_2$ | 11.3 | 9.7 | 8.5 | 7.5 | 6.6 | 5.9 | 5.3 |
| | $H/S$ | 10.4 | 9.0 | 7.8 | 6.9 | 6.1 | 5.4 | 4.9 |

## References

[1]   M. C. Knapp and P. M. Woodward, *J. Solid State Chem,* 2006, **179**, 1076–1085.

[2]   Q. Liu, X. B. Li, B. Zhang, L. X. Wang, Q. T. Zhang and L. Zhang, *Ceram. Int*. 2016, **42**, 15294–15300.